Probabilistic Risk Evaluation of Microgrids Considering Stability and Reliability

Song, Yubo; Sahoo, Subham; Yang, Yongheng; Blaabjerg, Frede

Published in:
IEEE Transactions on Power Electronics

DOI (link to publication from Publisher):
10.1109/TPEL.2023.3278037

Publication date:
2023

Document Version
Accepted author manuscript, peer reviewed version

Probabilistic Risk Evaluation of Microgrids Considering Stability and Reliability

Yubo Song, *Student Member*, *IEEE*, Subham Sahoo, *Senior Member*, *IEEE*, Yongheng Yang, *Senior Member*, *IEEE*, and Frede Blaabjerg, *Fellow*, *IEEE*

***Abstract* – Microgrids are being developed with higher penetration of renewable energy sources (RES) and utilization of power electronics. The functionality of microgrids is normally measured by two indices, stability and reliability, which are highly influenced by system configuration and generation/load mission profiles. Although system-level modeling approaches have been proposed to evaluate both the said indices for microgrids, they are still considered independently due to the mismatch in their timescales. To this end, it limits the derivation of a comprehensive risk framework to exploit the interdependencies between stability and reliability. Hence, this article addresses this gap for the first time in the realm of microgrids by proposing a probabilistic risk framework by considering stability and reliability simultaneously. Long-timescale reliability are basically decomposed into shorter-timescale events, whereas stability is treated as probabilistic events to be integrated into the risk evaluation. This framework can quantify the operation risk of microgrids, thereby providing a more intuitive approach to the design of microgrids. To validate the ruggedness of the proposed framework, system stability and reliability are assessed and interpreted under experimental conditions.**

***Index Terms* – Power electronic systems, risk evaluation, AC Microgrids, stability, reliability.**

I. Introduction

Microgrid systems are being developed to accommodate the modern distributed loads and the increasing penetration of renewable energy sources (RES) [1]. Power semiconductors with high controllability have been used in many converters and have enabled miscellaneous ways of implementing power conversion [2]. However, such flexibility of microgrid systems is not only leading to various possibilities for power applications, but also yields operational uncertainties that might be disadvantageous. Different from traditional power systems, the modern microgrid systems employing power electronics are vulnerable to more diverse mission profiles, and thus might lead to more frequent appearances of system abnormalities and/or failures [3].

The work is supported mainly by the Reliable Power Electronic-Based Power System (REPEPS) project at Department of Energy, Aalborg University, as a part of the Villum Investigator Program funded by the Villum Foundation, Denmark, and in part by the National Natural Science Foundation of China through the project 52107212 and the Zhejiang Kunpeng Investigator Program. (*Corresponding authors: Yubo Song, Yongheng Yang*)

Yubo Song, Subham Sahoo and Frede Blaabjerg are with the Department of Energy, Aalborg University (AAU Energy), 9220 Aalborg East, Denmark. (e-mail: yuboso@energy.aau.dk; sssa@energy.aau.dk; fbl@energy.aau.dk)

Yongheng Yang is with the College of Electrical Engineering, Zhejiang University, 310027 Hangzhou, Zhejiang, China. (e-mail: yoy@zju.edu.cn)

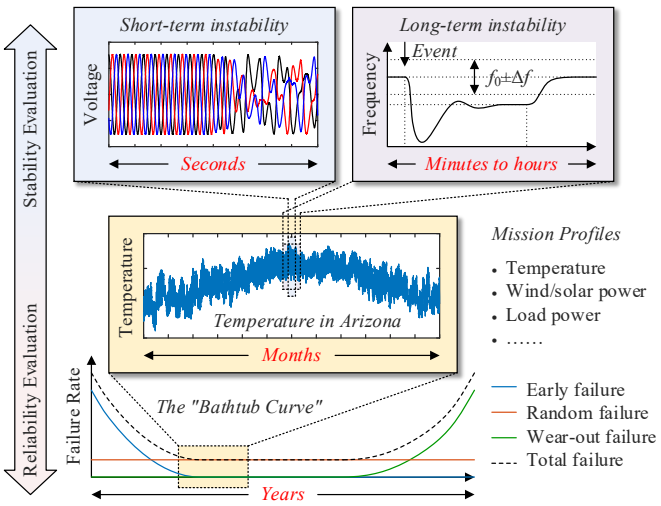

Fig. 1. Different timescales of stability and reliability evaluation of microgrids [7], [8], [17], [19], [20].

To measure the functionality of microgrid systems, reliability is introduced as the ability of a system to operate as per the requirement without failures [4]. The unreliability of the system can basically be regarded as kind of *operation risk*. Considering parameter uncertainties or the variation or heterogeneity of mission profiles, the failure of systems is a probabilistic event, reflecting the accumulation of stresses on the devices as like events over time. In the literature, the failure mechanisms of power electronics have been investigated in correlation with the design and planning of system operation, such that the overall lifetime of systems can be prolonged [5], [6].

On the other hand, stability is also an important performance criterion in microgrids [7], [8]. Differently from reliability which is a long-term performance, the time scale of stability analysis is relatively shorter, where state-space-based [9] and impedance-based approaches [10], [11] are widely used for stability modeling and analysis. Conventionally, system uncertainties are considered by analyzing the worst case and the boundary parameter values, wherein probabilistic stability is then introduced to accommodate these uncertainties and mismatch in the plant-control parameters [12]. In existing literature, the uncertainties can be modeled by Monte-Carlo-based methods, regression methods or neural networks, etc. [13], and probabilistic stability has been employed especially when quantifying the influences of parameter or mission profile uncertainties [14]-[16].

Meanwhile, it should be noted that stability is predominantly determined by the dynamic characteristic of a system, i.e., how the system instantly responds to a disturbance [17], instead of the accumulated damage. Thus, a system can be unstable, e.g., when there is a mismatch in the control and plant parameters, even if all devices are within lifetime [18]. Therefore, the reliability itself is not sufficient to represent the operation risk of a microgrid. In previous literature, the evaluation of stability and reliability is always implemented separately due to the large mismatch in their timescales, which is illustrated in Fig. 1. To this end, the system is assumed to be stable whilst evaluating its reliability [21], [22], and vice versa [9]-[11]. Nevertheless, both indices have collective impact on the performance of microgrids, wherein neither of them can be well reflected whilst the other is evaluated individually. They can also be coupling with each other when, e.g., parameter drift due to component degradation leads to instability, or harmonics due to parameter mismatch affect the stress on the components. Therefore, it should be more reasonable to consider both two indices simultaneously and determine a likely interdependency between them when evaluating the overall performance of microgrids, which is not addressed in existing literature.

This article thereby proposes a framework to evaluate the operation risk comprehensively considering the analysis of both stability and reliability simultaneously for the first time in the realm of power electronics and microgrids. The long-timescale reliability can be decomposed into events with smaller time frames, and the system can be stable in a certain probability in terms of system uncertainties. The system can be risky when either stability or reliability cannot be ensured, and the long-term risk is then evaluated by accumulating the small-time-frame events. Moreover, the *lifetime* of microgrid systems is also generalized in this article to match the proposed risk evaluation framework.

This article is organized as follows. Section II introduces the limitation of dissociating stability and reliability in microgrids. Section III further elaborates on the probability of stability and reliability in microgrid systems. Section IV proposes a comprehensive framework for system risk evaluation together with discussions on its applications. Experimental results are presented in Section V, demonstrating how stability and reliability are considered in the proposed framework. Finally, Section VI concludes the entire article.

II. Limitation of Dissociating Stability and Reliability in Microgrids

In this article, a three-phase AC microgrid system is selected as a study case, and it is shown in Fig. 2. The system consists of two DC-AC converters operating in parallel, and a resistive load is connected to the Point of Common Coupling (PCC). The power sharing between the two converters is implemented by *P-f* and *Q-V* droop controllers [23]. The key parameters of this system are listed in Table I.

It has been mentioned in Section I that stability and reliability should be considered simultaneously in practice, which is, specifically, instability could occur in reliable cases, and failures could also appear in stabilized systems due to the wear-out of components. Taking instability as an example, like in [17], several types of instability have been investigated based on the CIGRE low-voltage benchmark system, which could result from parameter mismatch, power inadequacy, or loss of synchronization, etc. A typical case is illustrated in Fig. 3. According to [9], a feed-forward gain F is normally adopted to the decoupling of grid-side current in cascaded voltage control loops of droop-based converters. In Fig. 3, the gain F of Converter 1 is decreased from 1 to 0.8, leading to frequency

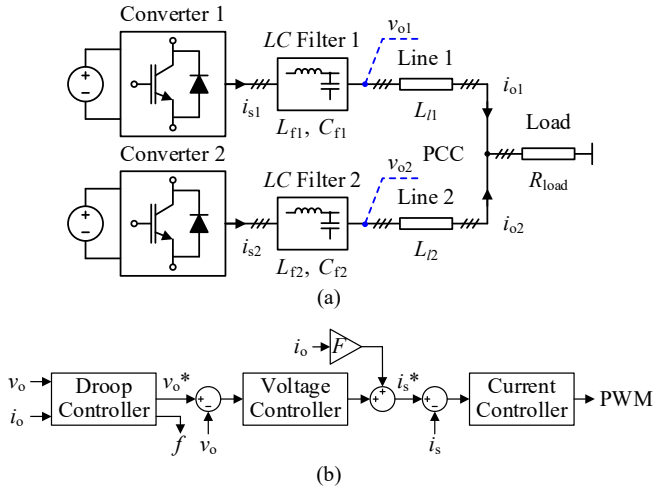

Fig. 2. (a) Layout of an example AC microgrid system, and (b) a brief control scheme. For each converter, L_f and C_f denote the parameters of the *LC* filter, and L_l denotes the parameter of the line, which is regarded as an inductance.

TABLE I
Key Parameters of the Two-Converter System

Parameters	Values
Nominal AC voltage V_n	110 V_{RMS}, 50 Hz
Switching frequency f_{sw}	10 kHz
LC Filter inductance L_{f1}, L_{f2}	$L_{f1} = L_{f2} = 2.0$ mH
LC Filter capacitance C_{f1}, C_{f2}	$C_{f1} = C_{f2} = 10$ μF
Line inductance L_{l1}, L_{l2}	$L_{l1} = L_{l2} = 0.5$ mH
Load resistance R_{load}	3 Ω (12 kW)
Base value of the *P–f* droop coefficient m_{p0}	9.4×10^{-5} [Hz/W]
Base value of the *Q–V* droop coefficient n_{q0}	1.3×10^{-3} [V/Var]

Note: V_{RMS} = Volts in Root-Mean-Square (RMS) value.

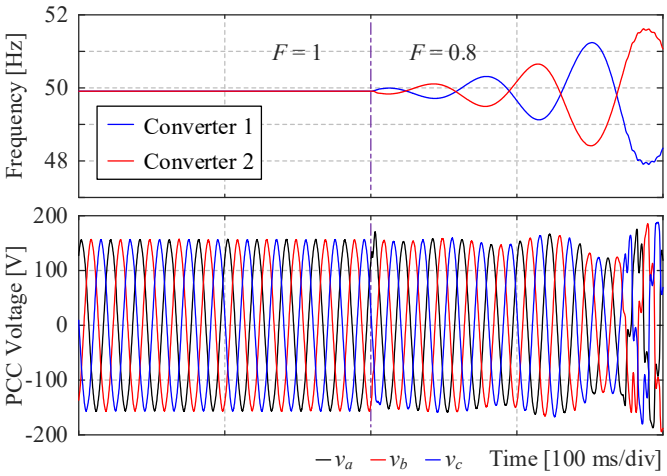

Fig. 3. Instability when the feedforward gain F for grid-side current decoupling in the cascaded double voltage loops of Converter 1 is decreased.

divergence and instability. As the feed-forward path counteracts the dynamics of the rest converters in the microgrid system, the decrease in F indicates stronger coupling between the two converters, but it has no impact on the power sharing relationship, and consequently no instant impact on the overall reliability due to the unaltered power flows. On the other hand, the triggered instability in Fig. 3 will still force a shutdown of the system as the divergence will eventually hit the threshold of system protection. Similar occasions could always happen when the system configuration changes over time, or the control parameters are modified to match the change of mission profiles.

In light of this, it is henceforth vital to take both stability and reliability into consideration simultaneously in order to achieve a more intuitive evaluation on the performance of a microgrid. Though the two indices are inconsistent in terms of timescales, the approach could be formalized by decomposing the long-timescale reliability into events with smaller time frames, where the probabilistic stability is a feasible tool to integrate the concept of stability into reliability analysis.

III. Probability of Stability and Reliability in Microgrid Systems

A. Probabilistic Stability of Microgrid Systems

Stability of a microgrid system measures how robust the system is in response to disturbances, and the system configurations make much difference herein [17]. To characterize the stability under certain system configurations, state-space-based and impedance-based modeling approaches are mostly employed [24].

In this article, the question is defined within controller-induced converter stability [7], [8], which is typical for droop-dominated microgrids. Hence, the example system is modeled by the state-space method that is similar to [9]. The dynamics of the double voltage loops and DC-link control loops are neglected for simplicity, and the small-signal state vector of the system can be obtained as $\Delta x_{\text{conv}}{}^{(k)}$:

$$\Delta \boldsymbol{x}_{\text{conv}}{}^{(k)} = \Delta\left[\delta^{(k)} \;\; P^{(k)} \;\; Q^{(k)} \;\; i_{\text{s}}{}^{(k)} \;\; v_{\text{o}}{}^{(k)} \;\; i_{\text{o}}{}^{(k)}\right]^{T} \tag{1}$$

where, k is 1 or 2 indicating the indices of converters, for each converter, δ is the phase angle for Park transformation, i_{s} and i_{o} are the current flowing through the filter inductor L_{f} and the line L_l, respectively, and v_{o} is the output voltage at the filter capacitor C_{f}. The load current is the sum of $i_{\text{o}1}$ and $i_{\text{o}2}$ according to the Kirchhoff's law, so the voltage at PCC (or the load voltage) is determined accordingly.

The state space model of the system can be obtained as:

$$\frac{\text{d}}{\text{d}t}\begin{bmatrix}\Delta \boldsymbol{x}_{\text{conv1}} \\ \Delta \boldsymbol{x}_{\text{conv2}}\end{bmatrix} = \boldsymbol{A}_{\text{MG}}\begin{bmatrix}\Delta \boldsymbol{x}_{\text{conv1}} \\ \Delta \boldsymbol{x}_{\text{conv2}}\end{bmatrix} \tag{2}$$

where, $\boldsymbol{A}_{\text{MG}}$ is the state matrix.

Based on the parameters in Table I, the eigenvalues of the state matrix $\boldsymbol{A}_{\text{MG}}$ can then be calculated as listed in Table II, where the droop gain is varied to identify the critical modes. In the state-space-based stability modeling, RHP eigenvalues will lead to system instability. It is shown in Table II that the conjugate eigenvalues λ_{11} and λ_{12} are located closest to the imaginary axis among the eigenvalues, which are sensitive to the parameter variation. Thus, it is reasonable to conclude that λ_{11} and λ_{12} are the critical modes in this case, which will be focused on in the rest of this section.

TABLE II
Eigenvalues of the System in Fig. 2

Index	Eigenvalues in default case	Eigenvalues when $m_{p1} = 2m_{p0}$
1, 2	–35.38 ± j16125	–35.38 ± j16125
3, 4	–34.60 ± j15497	–34.60 ± j15497
5, 6	–4735 ± j14527	–4735 ± j14527
7, 8	–4734 ± j13898	–4734 ± j13898
9, 10	–2740 ± j308.62	–2740 ± j308.62
11, 12	–1.17 ± j315.44	–1.10 ± j315.23
13	–0.32	–0.30
14	–61.29	–51.20 ± j5.68
15	–41.11	
16	–30.95	–31.10
17	–31.41	–31.41
18	–39.50	–39.50

In conventional stability analysis, microgrid systems are conventionally modeled in deterministic approaches. The system performances are evaluated based on specific scenarios, and the system variables are assumed to be deterministic, or in certain cases, time-invariant. However, in practice, it is always reasonable to take the system uncertainties into consideration, which may lead to the worst case of instability. This is especially critical when there is a small stability margin.

According to [12], the stability of microgrids may unexpectedly vary due to the uncertainty of operational conditions and disturbances. Operational conditions (variables) are typically the system internal configurations or parameters, while disturbances could be related to the external events, such as the mission profiles of RES. Mathematically, these variables can follow different probabilistic distributions (e.g., Gaussian distribution for the instantaneous load or power generation, and Poisson distribution for the fault incidents [12]), and the Monte-Carlo method can be a general approach to deal with most of those probabilistic distribution patterns. With this, only the probabilistic distributions of filter and line parameters are considered in this article without loss of generality, which are classified as operational variables, whereas the conclusions can be generalized by similarly applying Monte-Carlo method to other types of uncertainties that may cause instability as well.

In this article, the parameters of passive components in Fig. 2 (including the inductances and parasitic resistances of filter inductors and lines, and the capacitances of filter capacitors) are assumed to follow the Gaussian distribution, of which the Probability Density Function (PDF) can be expressed as:

$$f\left(X\right) = \frac{1}{\sigma_{\text{par}}\sqrt{2\pi}} \cdot \exp\left[-\frac{1}{2}\cdot\left(\frac{X-\mu_{\text{par}}}{\sigma_{\text{par}}}\right)^{2}\right] \tag{3}$$

where, X is an arbitrary parameter among the mentioned ones, μ_{par} is the mean value (or the nominal value) of the corresponding parameter, and σ_{par} is the standard deviation (the parameter error or uncertainty generally follows the 3-σ rule). It can also be denoted as $N\left(\mu_{\text{par}}, \sigma_{\text{par}}{}^{2}\right)$.

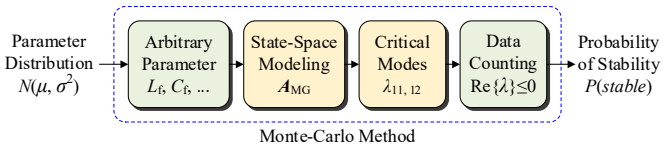

Fig. 4. Probabilistic evaluation of system stability.

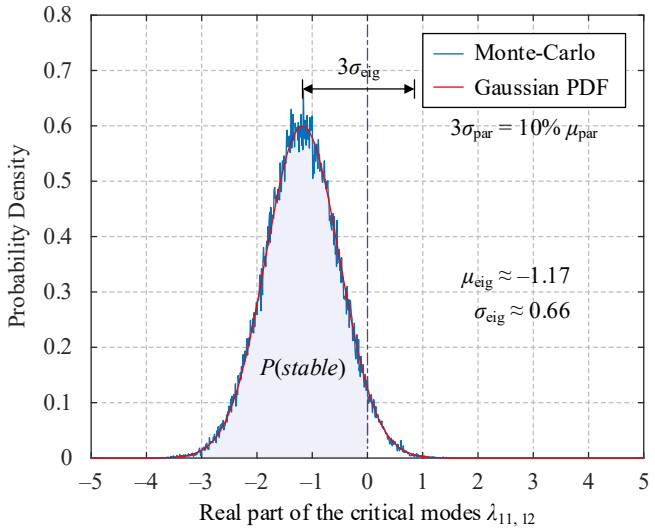

Fig. 5. Probability distribution of the real part of the critical modes, which mathematically follows the Gaussian distribution.

To simplify the analysis, it is also assumed that the uncertainties of all parameters are equal in per-unit value. In other words, the ratios of each standard deviation σ_{par} with respect to the corresponding mean value μ_{par} are assumed to be equal. Under this scenario, an example is first given with a parameter uncertainty of ±10%, where the standard deviation σ_{par} is 3.33% of μ_{par}. As the state matrix of the system is already constructed in (2), the probability distribution of the real part of critical modes can be obtained by repetitively calculating the eigenvalues with arbitrary parameter inputs, namely the Monte-Carlo method. The procedure is illustrated in Fig. 4.

***Remark 1*:** In this article, the parameters are assumed to be independent from each other. If, otherwise, certain parameters are supposed to be correlative, then the Monte-Carlo method can be conducted by sampling the variables in compatible groups instead.

***Remark 2*:** Generally, if there are k eigenvalues in total, all of them should be located in LHP to ensure system stability:

$$P(stable) = P\left(\bigcap_{j=1}^{k}\left\{\text{Re}\left\{\lambda_j\right\} \le 0\right\}\right) \tag{4}$$

As the real parts should be negative for uncritical modes, the analysis on critical modes is the simplified form of (4), as:

$$P(stable) = P\left(\text{Re}\left\{\lambda_{11,12}\right\} \le 0\right) = \int_{-\infty}^{0} f(\sigma)\,\text{d}\sigma \tag{5}$$

where f is the PDF of the real part of the critical modes. But if there are multiple critical modes with different real parts, or the critical modes vary over time, the simplification should be modified to include all critical modes accordingly.

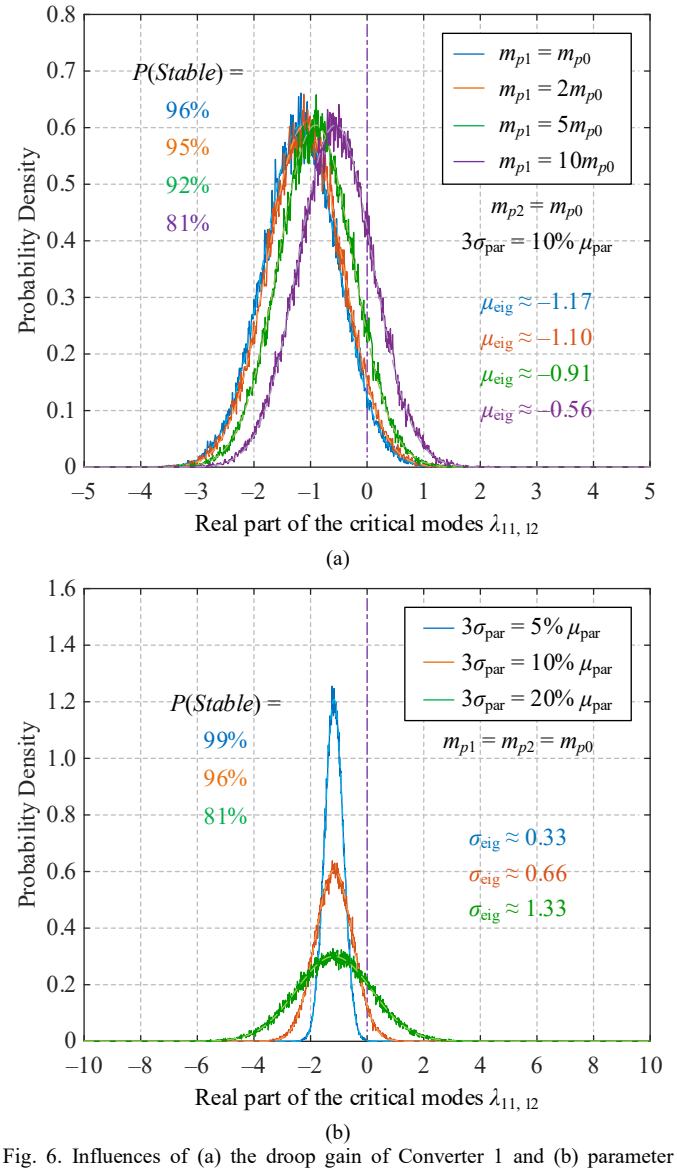

Fig. 6. Influences of (a) the droop gain of Converter 1 and (b) parameter uncertainty ($3\sigma_{par}$) on the probability distribution of the real part of the critical modes.

The probability density of the real part of the critical modes is plotted in Fig. 5. In this case, the real part of the critical modes follows the Gaussian distribution as well, which can be fitted by a Gaussian PDF as illustrated in Fig. 5. Most data fall into the 3σ region, namely the region of $[\mu_{\text{eig}}–3\sigma_{\text{eig}}, \mu_{\text{eig}}+3\sigma_{\text{eig}}]$, where μ_{eig} and σ_{eig} are respectively the mean value and standard deviation fit from Monte-Carlo validations. By excluding RHP eigenvalues which lead to system instability, the probability of system stability should be the area surrounded by the Gaussian density curve and the horizontal axis in the left-half plane (LHP), as highlighted in Fig. 5.

Accordingly, it can be discussed how the conventional deterministic stability analysis should be mapped to the case with system uncertainties. The influences of control parameters (droop gains) and parameter uncertainties on the real part of the critical modes are demonstrated in Fig. 6, also by Monte-Carlo method and Gaussian fitting. In Fig. 6(a), the variation of

control parameters leads to a horizontal shift of the probability distribution curve, where the mean value of the real part of the critical modes changes. In Fig. 6(b), the parameter uncertainty contributes to an increase of the standard deviation of the eigenvalues, and thus, the probability of stability changes accordingly.

***Remark 3*:** Differently from the conventional stability analysis where the uncertainty is zero, the probability of stability indicates that the system can still be unstable even if the mean value of the real part is negative.

***Remark 4*:** The probability of stability changes more significantly when the mean value is close to zero, or more specifically, when the vertical axis (zero) locates within the aforementioned 3σ region.

Furthermore, the comprehensive influence of the droop gain and parameter uncertainty on the probability of system stability can be summarized in Fig. 7. The probability of stability is the short-term operation risk of the system. It decreases consecutively with larger droop gains, where the conventional zero-uncertainty stable region corresponds to a 50% probability of stability. This results from the symmetry of the Gaussian distribution, and thus, it should be noted that the shape of these curves could change as the uncertainties increase with different probabilistic distribution patterns.

B. Reliability of Microgrid Systems

On the other hand, the reliability of a microgrid is assessed using a relatively long-term performance index, which also measures the functionality of the microgrid system. A system is reliable when it can perform its intended function without failure for a certain period, and the failures normally result from the degradation of components. Therefore, power semiconductors and capacitors among the most fragile components in power converters are the major focus in reliability analysis [25].

A cycle-based lifetime model of power semiconductors is given in (6) [26]. The average junction temperature T_{jm} and the swing of the junction temperature ΔT_{j} are the most decisive factors affecting the overall lifetime.

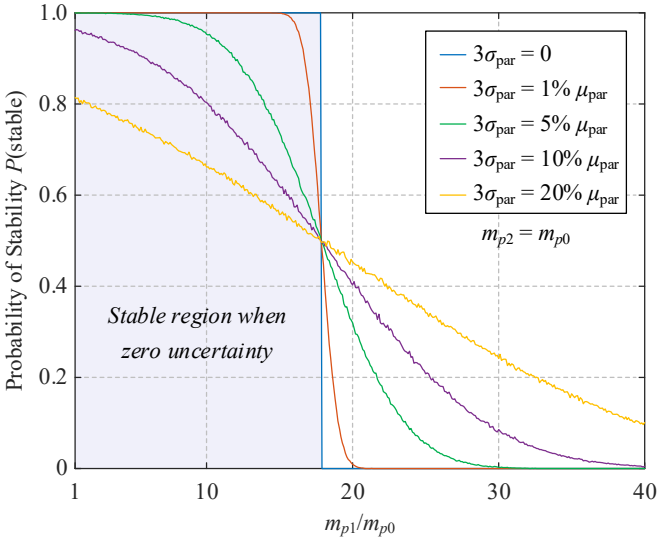

Fig. 7. Comprehensive influence of the droop gain and parameter uncertainty on the probability of system stability.

$$N_{\mathrm{f}} = A \cdot \Delta T_{\mathrm{j}}^{\alpha} \cdot \exp\left(\frac{\beta_1}{T_{\mathrm{jm}}}\right) \cdot t_{\mathrm{on}}{}^{\gamma} \tag{6}$$

where, A, α, β_1 and γ are the coefficients obtained by conducting the power-cycling tests like [27].

***Remark 5*:** This lifetime model is the most commonly used for power semiconductors, while it is also addressed in [28] that its accuracy is limited for cases with small ΔT_{j}. Nevertheless, this will not influence the validity of the basic idea of this article.

The lifetime of capacitors is calculated from its loading voltage V and temperature T [29]:

$$L = L_0 \cdot 2^{\frac{T_0 - T}{n_1}} \cdot \left(\frac{V}{V_0}\right)^{-n_2} \tag{7}$$

where, L_0 is the rated lifetime when the voltage is V_0 and the temperature is T_0. n_1 and n_2 are constant coefficients.

According to the Miner's rule [30], the accumulated damages of power semiconductors and capacitors are calculated by:

$$D_{\mathrm{sw}} = \sum_i \frac{n^{(i)}}{N_{\mathrm{f}}^{(i)}} \tag{8}$$

$$D_{\mathrm{cap}} = \sum_i \frac{\Delta t^{(i)}}{L^{(i)}} \tag{9}$$

where, (i) is used to denote the i-th time interval. In (8), n and N_{f} are, respectively, the number of power cycles obtained by rainflow counting and the expected cycles-to-failure. In (9), in the i-th time interval with duration $\Delta t^{(i)}$, the corresponding rated lifetime is $L^{(i)}$. The accumulated damage reaches 1 when the device is at its end of life (EOL), namely the entire lifetime.

For either a power semiconductor or a capacitor, its time-to-failure data follows the Weibull distribution over time, of which the Cumulative Density Function (CDF) is:

$$R(t) = \exp\left[-\left(\frac{t}{\eta}\right)^{\beta}\right] \tag{10}$$

where, β is the shaping parameter, and η is the characteristic lifetime. (8) and (9) basically yield the B_{10} lifetime, where there is an expectation of 10% of the device population that will fail to operate, or the time t when $R(t)$ equals 90%.

If there is no parallel path in the reliability block diagram [21], the reliability of a converter R_{conv} is the multiplication of all components inside. If there is no other fragile part and all converters are supposed to function well, the reliability of a microgrid R_{MG} is the multiplication of all converters inside. Those two relationships can be described as:

$$R_{\mathrm{conv}} = \prod_j R_{\mathrm{sw\ or\ cap}}{}^{(j)} \tag{11}$$

$$R_{\mathrm{MG}} = \prod_j R_{\mathrm{conv}}{}^{(j)} \tag{12}$$

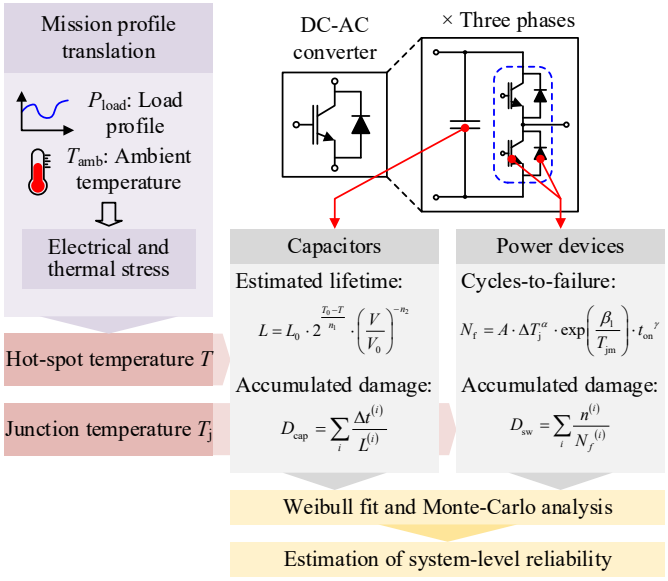

Fig. 8. Evaluation of the reliability in a three-phase DC-AC converter system.

Accordingly, the entire procedure is illustrated in Fig. 8. When there is an uncertainty of component parameters, the Monte-Carlo method can be similarly employed. The reliability is also describing the operation risk of the system, but physical failure mechanisms are considered here more than the mathematical mismatch of parameters.

In this article, the DC dynamics are not considered in the example system, and thus, only the degradation of power semiconductors is considered. The analysis procedure should be similar if the DC-link capacitors are also considered. For the case study, the types of power semiconductors in Converters 1 and 2 are chosen as Infineon FS25R12KT3 and FS35R12KT3, respectively, and then, the system-level reliability of the study case can be evaluated in Fig. 9. The power sharing between the two converters makes difference when the two converters are degrading at different rates. The unreliability reaches 1 by EOL, but the B_{10} lifetime is more critical for safe operation.

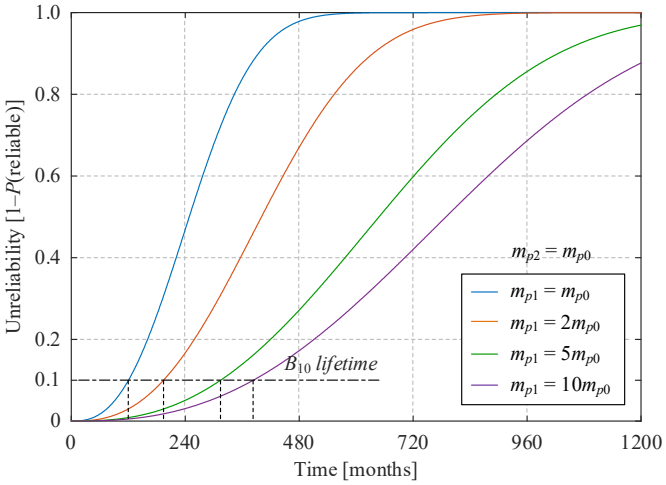

Fig. 9. System-level reliability evaluation of the example microgrid system when the power sharing between the two converters changes.

IV. Risk Evaluation Considering Probability of Stability and Reliability

The concept of risk in power systems is normally specified together with security. In [31], the risk is introduced as the probabilistic impact of unstable events, while in [32] and [33], a secure system without operation risk is required to be able to survive contingencies without service interruption. Similarly, both stability and reliability are considered in this article to include the abnormal events more comprehensively.

Different probabilistic relationships between stability and reliability are illustrated in Fig. 10 when analyzing the two indices. Fig. 10(a) and Fig. 10(b) represent the cases where one of the indices is constraining the other, which mathematically refers to conditional probability, but in terms of the operation risk of microgrids, instability and unreliability are functioning individually and jointly result in system failures, as shown in Fig. 10(c). Safe operation therein requires the intersection of stability and reliability.

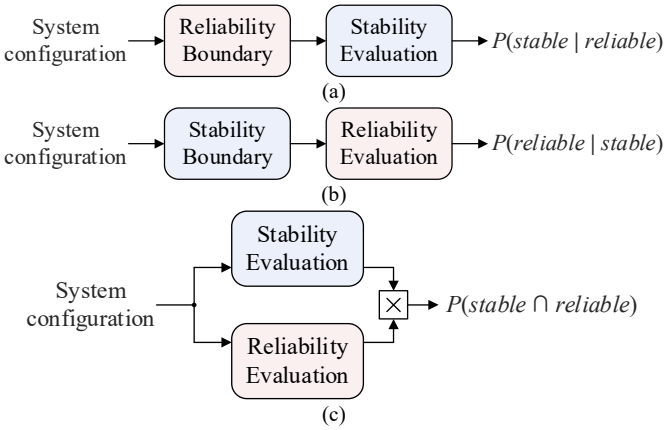

Fig. 10. Probabilistic relationship between stability and reliability analysis, which includes (a) reliability-constrained stability, (b) stability-constrained reliability, and (c) joint performance. The system configuration can basically include the topology and parameters of the studied system.

Accordingly, the probabilistic risk in this article is defined as:

Definition: *The probabilistic risk is the probability that a microgrid system cannot operate both stably and reliably to fulfil its expected function. The system is secure when the risk probability is sufficiently low.*

According to the definition, the risk should be calculated considering the probability of stability and reliability, and either unstable or unreliable events could lead to a nonzero risk. Therefore, the system operation risk can be calculated by the following probabilistic expression:

$$Risk = 1 - P\left(stable \cap reliable\right) \tag{13}$$

For the study case discussed in Sections II and III, the stability and reliability are mathematically independent for a certain system configuration Γ, namely:

$$Risk\big|_{\Gamma} = 1 - P\left(stable\right)\big|_{\Gamma} \cdot P\left(reliable\right)\big|_{\Gamma} \tag{14}$$

Based on (13) and (14), the framework of the operation risk in a microgrid system can be formalized as shown in Fig. 11. The system uncertainties influence the probability of stability,

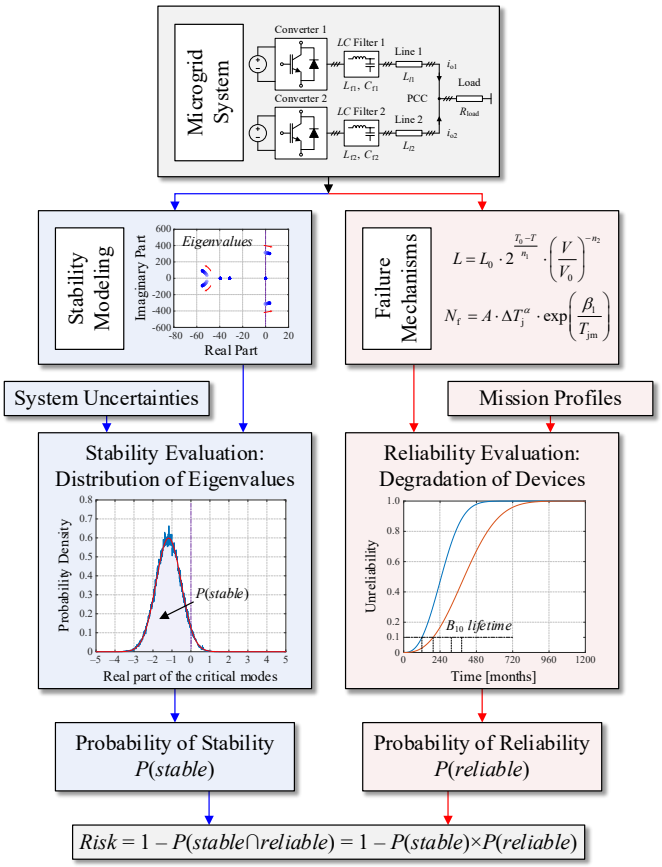

Fig. 11. Comprehensive framework of operation risk evaluation in a microgrid system considering both stability and reliability.

while the mission profiles are the major concern of device degradation. Both stability and reliability are contributing to the overall risk.

***Remark 6*:** In the study case, the uncertainties in stability analysis do not affect the evaluation of system reliability, which is based on the mission profiles and failure mechanisms, and vice versa. In other cases, the stability and reliability may not be independent from each other, and the overall operation risk should be the collection of all possible conditions. Monte-Carlo methods can be a practical approach to conduct the analysis.

***Remark 7*:** In this article, it is also assumed that the probability of stability does not change over time. For example, if the degradation of passive components has much influence on system eigenvalues, the system risk may need to be discussed in a piecewise way, where the probability of stability is a Markov variable dependent on instantaneous system configurations.

Based on Fig. 11, the long-term operation risk of the example system is demonstrated in Fig. 12. Compared with the reliability curves in Fig. 9, the risk considering both stability and reliability is higher from the beginning, indicating a non-zero risk due to the parameter uncertainties. Besides, when the droop parameters are varied to implement a power sharing relationship with higher system-level reliability, the probability of stability might contrarily decrease the overall operation risk. Therefore, it is of significance to seek for a trade-off between

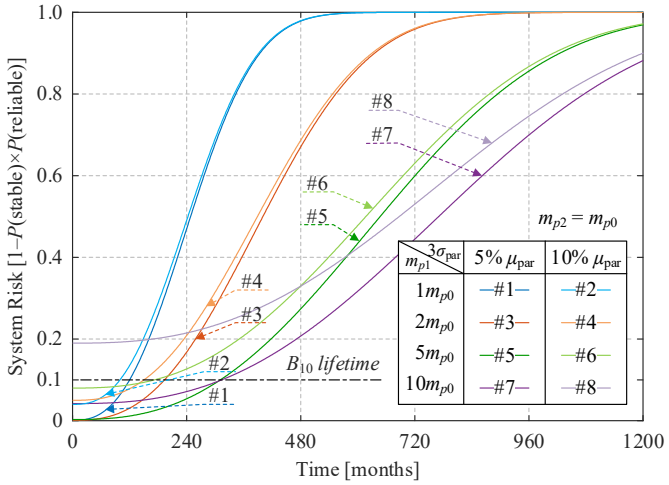

Fig. 12. Long-term operation risk of the example microgrid system in Fig. 2.

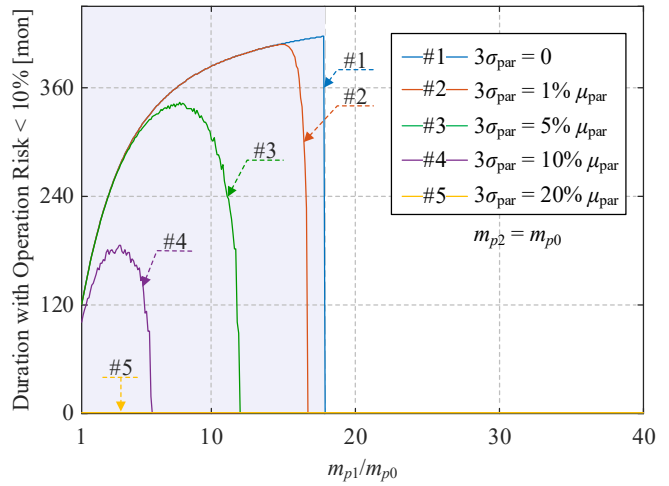

Fig. 13. Influence of control parameters and system uncertainties on the low-risk (less than 10%) time span of the example microgrid system.

stability and reliability and the overall optimal operation point in the design and planning of microgrids.

In reliability analysis, there is a concept of B_{10} lifetime which denotes the time span when the system can operate highly safely. In Fig. 12, however, if we generalize the B_{10} lifetime to the time span where the system risk is below 10%, the lifetime will be shorter due to the consideration of stability. There are also cases (e.g., Curve #8) where the lifetime equals zero, or the current design cannot ensure an operation risk below 10%.

In Fig. 13, such lifetime is calculated and summarized in terms of the droop gain m_{p1} and system uncertainty. All curves appear within the stable region same as Fig. 7, indicating that the stability of the system is the preliminary boundary of the safety operation. By identifying the local maximum in the Curves #1-4, the theoretical maximum generalized B_{10} *lifetime* under different scenarios and the corresponding optimal power sharing can be achieved, which is practical in the system design.

Similar to Fig. 12, it should also be noted that, the operation risk of the system can sometimes be above the 10% limit, like Curve #5 in Fig. 13, such that the variation of control parameters makes no difference. This should be specially noted in system design to avoid potential system failures.

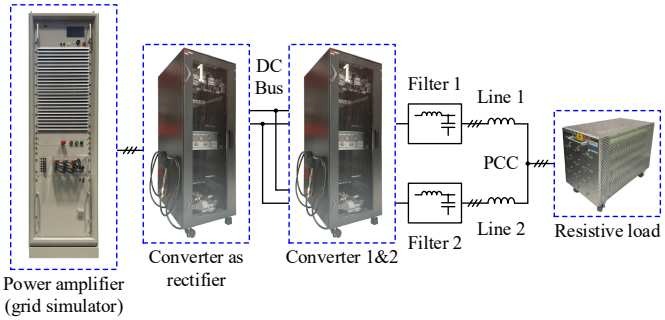

Fig. 14. Configuration of the experimental setup. Two three-phase DC-AC converters are installed in each converter rack.

V. Validations with Results

In this section, tests are performed to demonstrate how stability and reliability are reflected in the proposed framework. The experimental setup is shown in Fig. 14, of which the topology is similar to that in Fig. 2. Two 7-kW DC-AC converters are connected in parallel, and inductors are used as the line impedances. In the experiments, the load is downscaled to 57 Ω due to the available hardware, and the parameter uncertainty is simulated by varying the inductors in Filters 1 and 2, but long-term analysis is conducted by assuming a 12-kW load as mentioned in Table I, corresponding to the selected types of power semiconductors and without loss of generality. Other parameters are the same as those listed in Table I.

A. Stability Consideration in the Proposed Framework

A basic case is illustrated with equal inductance in Filters 1 and 2. Based on the available hardware, the filter inductors are changed from 1.0 mH/40 mΩ to 0.86 mH/27.1 mΩ and 0.6 mH/21.6 mΩ to emulate a parameter uncertainty (14% and 40%, respectively, compared to the initial value), and 1.2 mH/39.6 mΩ and 1.5 mH/47 mΩ as supplementary illustrations for stable cases. Experimental results are then shown in Fig. 15. In Fig. 15(b), an increase in harmonics can be observed, while in Fig. 15(c), the harmonics turn into serious loss of stability with current distortion. Though the load voltage is not influenced significantly in this case, such distortion is more likely to grow into a system failure when there are heterogeneous controllers and dynamics in a larger multi-converter microgrid.

The proposed risk evaluation is then performed with regard to this case, and the results are presented in Table III. The decrease in inductance has led to less stability in the experimental results, and meanwhile, it accords with the decrease in probability of stability in Table III. Similarly, both the estimated 10%- and 20%- risk lifetimes decrease

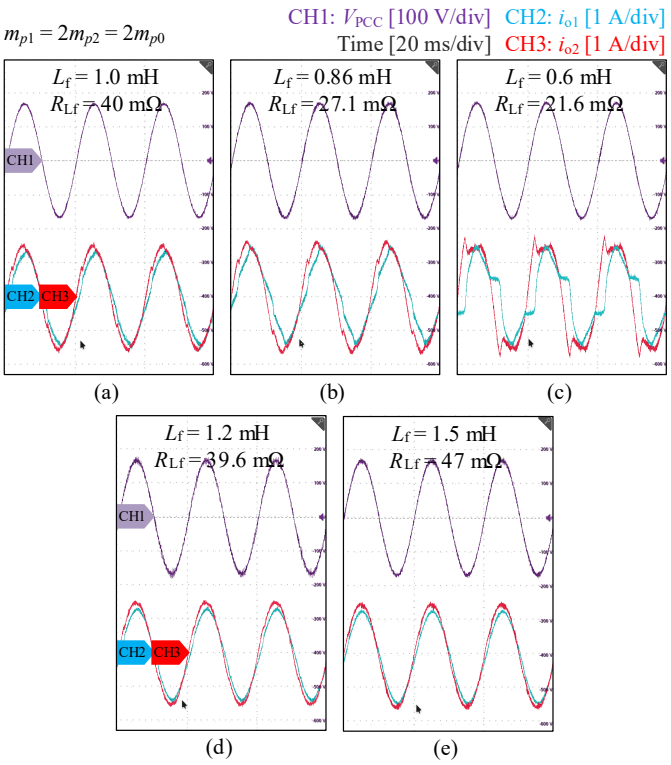

Fig. 15. Experimental results when there is a variation in both two filter inductors, with the value of (a) 1.0 mH/40 mΩ, (b) 0.86 mH/27.1 mΩ, (c) 0.6 mH/21.6 mΩ, (d) 1.2 mH/39.6 mΩ, and (e) 1.5 mH/47 mΩ. The cases (a)-(c) are analyzed in details to emulate a parameter uncertainty.

significantly when the system is less likely to be stable, and the instability plays a more decisive role herein. Therefore, it can be concluded that system stability has been considered in the proposed framework.

Besides, the experimental results in Fig. 15 have also shown that, the system can be unstable even if there is no component failure, or when the system is reliable: the instability is only caused by parameter mismatch and the system is restorable. This conclusion also emphasizes the significance of designing and planning the operation of microgrid systems with both stability and reliability considered.

B. Reliability Consideration in the Proposed Framework

To validate the reliability consideration in the proposed framework, the droop gain of Converter 1 m_{p1} is varied from m_{p0} up to $10m_{p0}$, and the types of power semiconductors accord with those mentioned in Section III-B. With the load being 12 kW, the power sharing between the two converters will change as listed in Table IV, subsequently achieving different lifetime expectation and reliability performance.

TABLE III
System Risk Evaluation under the Example Conditions

Inductance of *LC* filters [mH]	Inductance deviation [% of μ_{par}]	Probability of stability *P*(stable)	Estimated 10%-risk lifetime [months]	Estimated 20%-risk lifetime [months]
1.0 mH	0%	100%	194	259
0.86 mH	14%	88.57%	0	191
0.6 mH	40%	66.09%	0	0

TABLE IV
Power Sharing under the Example Conditions

Ratio of the droop gains [m_{p1}/m_{p2}]	Loading of Converter 1 [kW]	Loading of Converter 2 [kW]
1	5.79	5.79
2	5.53	6.05
5	5.26	6.31
10	5.14	6.43

Based on this, the unreliability curve is plotted in Fig. 16, which also accords with Fig. 9. Since the power semiconductors in Converter 2 has higher power rating, the system reliability can be improved, and the lifetime is accordingly extended.

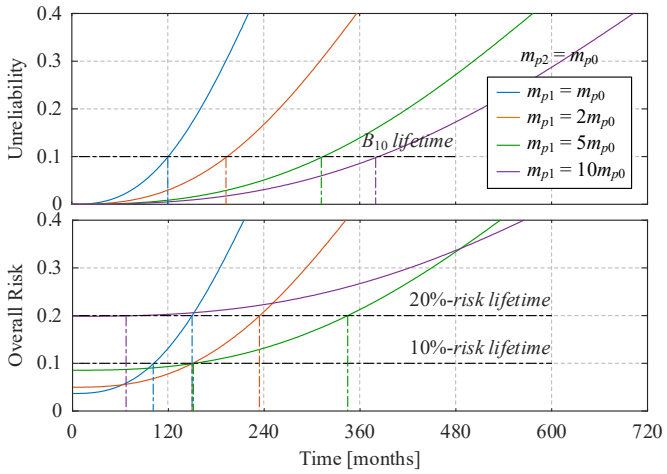

Fig. 16. Unreliability curve and the overall operation risk of the system under different droop gains.

Meanwhile, the system risk is also evaluated based on the parameter variation, as also shown in Fig. 16, and the results are summarized in Table V, supposing that a 10% uncertainty is assumed for evaluating the probability of stability. The estimated 10%- and 20%- risk lifetimes accord with the B_{10} lifetime when system uncertainty is zero, which shows that reliability is also well considered in the proposed framework.

TABLE V
SYSTEM RISK EVALUATION UNDER THE EXAMPLE CONDITIONS

Ratio of the droop gains [m_{p1}/m_{p2}]	B_{10} lifetime w/o considering uncertainties [months]	Probability of stability with 10% uncertainty	Estimated 10%-risk lifetime [months]	Estimated 20%-risk lifetime [months]
1	120	96.33%	101	149
2	194	95.01%	150	234
5	314	91.45%	152	344
10	383	80.14%	0	79

However, the increase in droop gains makes difference not only in power distribution, but also in the probability of stability. When the droop gain m_{p1} is further increased to $10m_{p0}$, the stability will play a dominant role in the system risk. Such case cannot be easily discovered through conventional reliability evaluation, yet the proposed framework could still reveal this issue, and appears more comprehensive and instructive in the system design.

VI. CONCLUSIONS AND FUTURE SCOPE OF WORK

In this article, a comprehensive framework for operation risk evaluation in microgrid systems is proposed for the first time, incorporating probabilistic methods for simultaneous assessment of stability and reliability. Both stability and reliability imply on a significant difference in the performance of microgrid systems, and the proposed framework combines the two performances mathematically by decomposing the long-timescale reliability into shorter-timescale events and integrating stability by probabilistic approaches. Accordingly, the concept of *lifetime* can be generalized and used to help identify the optimal operation point and design of the system. The proposed framework is tested under different test cases to highlight the risk modeling integrity and probabilistic estimation to anticipate stability and reliability risks during network expansion of microgrids.

In practice, taking both stability and reliability into consideration can provide a more encyclopedic insight of operation risk of microgrid systems, which is not fully focused on in existing research. The generalized *lifetime* can also describe the operation risk more intuitively for microgrid systems. In the future, to extend the scope of this article, there can be more centered discussion in terms of the assumptions applied, e.g., the probabilistic stability related to component degradation and parameter variation, and the systems with multiple critical modes. It should also be pragmatic that the probabilistic relationship between stability and reliability can further be formalized based on the Bayesian inference and accordingly characterized with machine-learning tools.

REFERENCES

[1] D. Boroyevich, I. Cvetković, D. Dong, R. Burgos, F. F. Wang, and F. C. Lee, "Future Electronic Power Distribution Systems - A Contemplative View," in *Proc. OPTIM 2010*, Brasov, Romania, May 2010, pp. 1369-1380.

[2] J. M. Carrasco, L. G. Franquelo, J. T. Bialasiewicz, E. Galván, R. C. P. Guisado, M. Á. M. Prats, J. I. León, and N. Moreno-Alfonso, "Power-Electronic Systems for the Grid Integration of Renewable Energy Sources: A Survey," *IEEE Trans. Ind. Electron.*, vol. 53, no. 4, pp. 1002-1016, Aug. 2006.

[3] J. Falck, C. Felgemacher, A. Rojko, M. Liserre, and P. Zacharias, "Reliability of Power Electronics Systems: An Industry Perspective," *IEEE Ind. Electron. Mag.*, vol. 12, no. 2, pp. 24-35, Jun. 2018.

[4] S. Peyghami, P. Palensky, and F. Blaabjerg, "An Overview on the Reliability of Modern Power Electronic Based Power Systems," *IEEE Open J. Power Electron.*, vol. 1, pp. 34-50, Feb. 2020.

[5] H. Wang, M. Liserre, F. Blaabjerg, P. d. P. Rimmen, J. B. Jacobsen, T. Kvisgaard, and J. Landkildehus, "Transitioning to Physics-of-Failure as a Reliability Driver in Power Electronics," *IEEE J. Emerging Sel. Top. Power Electron.*, vol. 2, no. 1, pp. 97-114, Mar. 2014.

[6] R. Burgos, G. Chen, F. F. Wang, D. Boroyevich, W. G. Odendaal, and J. D. van Wyk, "Reliability-Oriented Design of Three-Phase Power Converters for Aircraft Applications," *IEEE Trans. Aerosp. Electron. Syst.*, vol. 48, no. 2, pp. 1249-1263, Apr 2012.

[7] M. Farrokhabadi, C. A. Canizares, J. W. Simpson-Porco, E. Nasr, L. Fan, P. A. Mendoza-Araya, R. Tonkoski, U. Tamrakar, N. Hatziargyriou, D. Lagos, R. W. Wies, M. Paolone, M. Liserre, L. Meegahapola, M. Kabalan, A. H. Hajimiragha, D. Peralta, M. A. Elizondo, K. P. Schneider, F. K. Tuffner, and J. Reilly, "Microgrid Stability Definitions, Analysis, and Examples," *IEEE Trans. Power Syst.*, vol. 35, no. 1, pp. 13-29, Jan. 2020.

[8] N. Hatziargyriou, J. V. Milanovic, C. Rahmann, V. Ajjarapu, C. Cañizares, I. Erlich, D. Hill, I. Hiskens, I. Kamwa, B. Pal, P. Pourbeik, J. Sanchez-Gasca, A. Stankovic, T. Van Cutsem, V. Vittal, and C. Vournas, "Definition and Classification of Power System Stability – Revisited & Extended," *IEEE Trans. Power Syst.*, vol. 36, no. 4, pp. 3271-3281, Jul. 2021.

[9] N. Pogaku, M. Prodanovic, and T. C. Green, "Modeling, Analysis and Testing of Autonomous Operation of an Inverter-Based Microgrid," *IEEE Trans. Power Electron.*, vol. 22, no. 2, pp. 613-625, Mar. 2007.

[10] J. Sun, "Impedance-Based Stability Criterion for Grid-Connected Inverters," *IEEE Trans. Power Electron.*, vol. 26, no. 11, pp. 3075-3078, Nov. 2011.

[11] X. Wang, F. Blaabjerg, and W. Wu, "Modeling and Analysis of Harmonic Stability in an AC Power-Electronics-Based Power System," *IEEE Trans. Power Electron.*, vol. 29, no. 12, pp. 6421-6432, Dec. 2014.

[12] K. N. Hasan, R. Preece, and J. V. Milanovic, "Existing Approaches and Trends in Uncertainty Modelling and Probabilistic Stability Analysis of Power Systems with Renewable Generation," *Renewable Sustainable Energy Rev.*, vol. 101, pp. 168-180, Mar. 2019.
[13] A. M. Hakami, K. N. Hasan, M. Alzubaidi, and M. Datta, "A Review of Uncertainty Modelling Techniques for Probabilistic Stability Analysis of Renewable-Rich Power Systems," *Energies*, vol. 16, no. 1, Dec. 2022.
[14] R. Preece, N. C. Woolley, and J. V. Milanovic, "The Probabilistic Collocation Method for Power-System Damping and Voltage Collapse Studies in the Presence of Uncertainties," *IEEE Trans. Power Syst.*, vol. 28, no. 3, pp. 2253-2262, Aug. 2013.
[15] W. Chen, X. Xie, D. Wang, H. Liu, and H. Liu, "Probabilistic Stability Analysis of Subsynchronous Resonance for Series-Compensated DFIG-Based Wind Farms," *IEEE Trans. Sustainable Energy*, vol. 9, no. 1, pp. 400-409, Jan. 2018.
[16] K. Ye, J. Zhao, N. Duan, and Y. Zhang, "Physics-Informed Sparse Gaussian Process for Probabilistic Stability Analysis of Large-Scale Power System with Dynamic PVs and Loads," *IEEE Trans. Power Syst.*, vol. 38, no. 3, pp. 2868-2879, May 2023.
[17] Y. Song, S. Sahoo, Y. Yang, and F. Blaabjerg, "System-Level Stability of the CIGRE Low Voltage Benchmark System: Definitions and Extrapolations," in *Proc. 2021 IEEE COMPEL*, Cartagena, Colombia, Nov. 2021, pp. 1-6.
[18] Y. Song, S. Sahoo, Y. Yang, and F. Blaabjerg, "Stability Constraints on Reliability-Oriented Control of AC Microgrids – Theoretical Margin and Solutions," *IEEE Trans. Power Electron.*, 2023, early access.
[19] J. Fang, H. Li, Y. Tang, and F. Blaabjerg, "On the Inertia of Future More-Electronics Power Systems," *IEEE J. Emerging Sel. Top. Power Electron.*, vol. 7, no. 4, pp. 2130-2146, Dec. 2019.
[20] D. Zhou, G. Zhang, and F. Blaabjerg, "Optimal Selection of Power Converter in DFIG Wind Turbine with Enhanced System-Level Reliability," *IEEE Trans. Ind. Appl.*, vol. 54, no. 4, pp. 3637-3644, Jul./Aug. 2018.
[21] D. Zhou, H. Wang, and F. Blaabjerg, "Mission Profile Based System-Level Reliability Analysis of DC/DC Converters for a Backup Power Application," *IEEE Trans. Power Electron.*, vol. 33, no. 9, pp. 8030-8039, Sept. 2018.
[22] S. Peyghami, H. Wang, P. Davari, and F. Blaabjerg, "Mission-Profile-Based System-Level Reliability Analysis in DC Microgrids," *IEEE Trans. Ind. Appl.*, vol. 55, no. 5, pp. 5055-5067, Sept./Oct. 2019.
[23] J. Rocabert, A. Luna, F. Blaabjerg, and P. Rodríguez, "Control of Power Converters in AC Microgrids," *IEEE Trans. Power Electron.*, vol. 27, no. 11, pp. 4734-4749, Nov. 2012.
[24] Y. Song, S. Sahoo, Y. Yang, and F. Blaabjerg, "Quantitative Mapping of Modeling Methods for Stability Validation in Microgrids," *IEEE Open J. Power Electron.*, vol. 3, pp. 679-688, Oct. 2022.
[25] S. Yang, A. Bryant, P. Mawby, D. Xiang, L. Ran, and P. Tavner, "An Industry-Based Survey of Reliability in Power Electronic Converters," *IEEE Trans. Ind. Appl.*, vol. 47, no. 3, pp. 1441-1451, May/Jun. 2011.
[26] R. Bayerer, T. Herrmann, T. Licht, J. Lutz, and M. Feller, "Model for Power Cycling Lifetime of IGBT Modules - Various Factors Influencing Lifetime," in *Proc. 5th International Conference on Integrated Power Electronics Systems*, Nuremberg, Germany, Mar. 2008, pp. 1-6.
[27] Infineon. AN2019-05: PC and TC Diagrams, Rev. 2.1, Feb. 2021. Accessed: Apr. 2022. [Online] Available: https://www.infineon.com/dgdl/Infineon-AN2019-05_PC_and_TC_Diagrams-ApplicationNotes-v02_01-EN.pdf?fileId=5546d46269e1c019016a594443e4396b
[28] J. Lutz, C. Schwabe, G. Zeng and L. Hein, "Validity of Power Cycling Lifetime Models for Modules and Extension to Low Temperature Swings," in *Proc. EPE'20 ECCE Europe*, Lyon, France, 2020, pp. P.1-P.9.
[29] H. Wang and F. Blaabjerg, "Reliability of Capacitors for DC-Link Applications in Power Electronic Converters - An Overview," *IEEE Trans. Ind. Appl.*, vol. 50, no. 5, pp. 3569-3578, Sep.-Oct. 2014.
[30] M. A. Miner, "Cumulative Damage in Fatigue," *J. Appl. Mech.*, vol. 12, no. 3, pp. A159-A164, 1945.
[31] J. D. McCalley, A. A. Fouad, V. Vittal, A. A. Irizarry-Rivera, B. L. Agrawal, and R. G. Farmer, "A Risk-Based Security Index for Determining Operating Limits in Stability-Limited Electric Power Systems," *IEEE Trans. Power Syst.*, vol. 12, no. 3, pp. 1210-1219, Aug. 1997.
[32] CIGRE Task Force 38.03.12. "Power System Security Assessment: A Position Paper," *Electra*, vol. 175, pp. 49-77, 1997.
[33] K. Morison, L. Wang, and P. Kundur, "Power System Security Assessment," *IEEE Power Energy Mag.*, vol. 2, no. 5, pp. 30-39, Sept.-Oct. 2004.

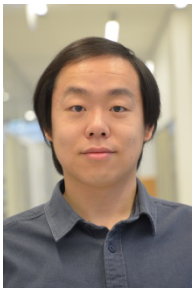

Yubo Song (S'18) received the B.Sc. and M.Eng. degrees in Electrical Engineering from Shanghai Jiao Tong University, Shanghai, China, in 2016 and 2019, respectively. He is currently working toward Ph.D. degree in the Department of Energy, Aalborg University (AAU Energy), Aalborg, Denmark.

From May to July 2022, he was a visiting researcher with the University of Alberta, Edmonton, AB, Canada.

His research interests include the control, stability and reliability of power electronic systems.

Subham Sahoo (S'16–M'18–SM'23) received the B.Tech. & Ph.D. degree in Electrical and Electronics Engineering from VSSUT, Burla, India and Electrical Engineering at Indian Institute of Technology, Delhi, New Delhi, India in 2014 & 2018, respectively. He is currently an Assistant Professor in the Department of Energy, Aalborg University (AAU), Denmark, where he is also the vice-leader of the research group on Reliability of Power Electronic Converters (ReliaPEC) in AAU Energy.

He is a recipient of the Indian National Academy of Engineering (INAE) Innovative Students Project Award for the best PhD thesis across all the institutes in India for the year 2019. He is selected into EU-US National Academy of Engineering (NAE) Frontier of Engineering (FOE) Class of 2021. He was also a distinguished reviewer for IEEE TRANSACTIONS ON SMART GRID in 2020. He is currently the vice-chair of IEEE PELS Technical Committee (TC) 10 on Design Methodologies. He is an Associate Editor on IEEE TRANSACTIONS ON TRANSPORTATION ELECTRIFICATION.

His research interests are control, optimization, cybersecurity and stability of power electronic dominated grids, application of artificial intelligence and machine learning in power electronic systems.

Yongheng Yang (SM'17) earned his B.Eng. degree in Electrical Engineering and Automation from Northwestern Polytechnical University, China, in 2009, and his Ph.D. degree in energy technology from Aalborg University, Denmark, in 2014.

He pursued postgraduate studies at Southeast University, China, from 2009 to 2011 and was a Visiting Scholar at Texas A&M University, USA, during March-May 2013. From 2014 to 2020, he was associated with the Department of Energy Technology at Aalborg University, where he achieved the rank of tenured Associate Professor in 2018. In January 2021, he joined Zhejiang University in China as a ZJU100 Professor. He became a Zhejiang Kunpeng Investigator in 2023. His research focuses on grid-integration of photovoltaic systems and control of power converters, specifically grid-forming control technologies.

Dr. Yang served as the Chair of the IEEE Denmark Section in 2019-2020 and is an Associate Editor for several IEEE Transactions. He received the 2018 IET Renewable Power Generation Premium Award and was recognized as an Outstanding Reviewer for the IEEE Transactions on Power Electronics in 2018. He was the recipient of the

2021 Richard M. Bass Outstanding Young Power Electronics Engineer Award from the IEEE Power Electronics Society (PELS) and the 2022 IEEJ Isao Takahashi Power Electronics Award. In addition, he has received two IEEE Best Paper Awards. He was included on the list of the Highly Cited Chinese Researchers by Elsevier in 2022-2023. He is presently a Vice Chair of the IEEE PELS Technical Committee on Sustainable Energy Systems and a Council Member of the China Power Supply Society.

Frede Blaabjerg (S'86–M'88–SM'97–F'03) received the Ph.D. degree in electrical engineering from Aalborg University, Aalborg, Denmark, in 1995.

He was with ABB-Scandia, Randers, Denmark, from 1987 to 1988. He became an Assistant Professor in 1992, an Associate Professor in 1996, and a Full Professor of power electronics and drives in 1998. From 2017 he became a Villum Investigator. He is *honoris causa* at University Politehnica Timisoara (UPT), Romania, in 2017, and Tallinn Technical University (TTU) in Estonia, in 2018. His current research interests include power electronics and its applications, such as in wind turbines, PV systems, reliability, harmonics, and adjustable speed drives. He has published more than 600 journal papers in the fields of power electronics and its applications. He is the co-author of four monographs and editor of ten books in power electronics and its applications.

He has received 32 IEEE Prize Paper Awards, the IEEE PELS Distinguished Service Award in 2009, the EPE-PEMC Council Award in 2010, the IEEE William E. Newell Power Electronics Award 2014, the Villum Kann Rasmussen Research Award 2014, the Global Energy uPrize in 2019 and the 2020 IEEE Edison Medal. He was the Editor-in-Chief of the IEEE TRANSACTIONS ON POWER ELECTRONICS from 2006 to 2012. He has been a Distinguished Lecturer for the IEEE Power Electronics Society from 2005 to 2007 and for the IEEE Industry Applications Society from 2010 to 2011 as well as 2017 to 2018. In 2019-2020 he served as President of the IEEE Power Electronics Society. He is Vice-President of the Danish Academy of Technical Sciences too. He is nominated in 2014-2019 by Thomson Reuters to be between the most 250 cited researchers in Engineering in the world.